Synthesis, Sintering, and Electrical Properties of $BaCe_{0.9-x}Zr_xY_{0.1}O_{3-\delta}$

Sandrine Ricote, Gilles Caboche, Claude Estournès, Nikolaos Bonanos

Hindawi Publishing Corporation
Journal of Nanomaterials
Volume 2008, Article ID 354258, 5 pages
doi:10.1155/2008/354258

Research Article

Synthesis, Sintering, and Electrical Properties of $BaCe_{0.9-x}Zr_xY_{0.1}O_{3-\delta}$

S. Ricote,[1] G. Caboche,[1] C. Estournes,[2] and N. Bonanos[3]

[1] *Institut Carnot de Bourgogne, CNRS UMR 5209, Université de Bourgogne, 9 avenue Alain Savary, 21078 Dijon Cedex, France*
[2] *Plateforme Nationale de Frittage Flash (PNF2) et CIRIMAT UMR5085 CNRS/UPS/INPT, Université Paul Sabatier, 118 route de Narbonne, 31062 Toulouse Cedex 04, France*
[3] *Risø National Laboratory for Sustainable Energy, Fuel Cells and Solid State Chemistry Division, Technical University of Denmark, P.O. Box 49, 4000 Roskilde, Denmark*

Correspondence should be addressed to S. Ricote, sandrine.ricote@risoe.dk

Received 26 October 2007; Revised 9 May 2008; Accepted 2 September 2008

Recommended by Wanqin Jin

$BaCe_{0.9-x}Zr_xY_{0.1}O_{3-\delta}$ powders were synthesized by a solid-state reaction. Different contents of cerium and zirconium were studied. Pellets were sintered using either conventional sintering in air at 1700°C or the Spark Plasma Sintering (SPS) technique. The density of the samples sintered by SPS is much higher than by conventional sintering. Higher values of ionic conductivity were obtained for the SPS sample.

1. INTRODUCTION

Fuel cells can exhibit high-energy efficiency, and the only release is clean water when used with hydrogen. Types of fuel cells are classified according to the electrolyte material. Solid electrolytes are used in solid oxide fuel cell (SOFC). In that case, the electrolyte conducts oxygen ions from the cathode to the anode where they react chemically with hydrogen to form water. Oxygen diffusion occurs at roughly 800–900°C for YSZ [1, 2]. In order to lower the operating temperature, it is interesting to use a proton-conducting ceramic [2, 3]. This kind of fuel cell is called protonic ceramic fuel cell (PCFC). In that case, protons pass through the electrolyte to combine with oxygen at the cathode to liberate water. Hydrogen transport requires lower temperatures than oxygen transport.

Many rare-earth-doped perovskite materials seem to be good candidates for this application, because of their high proton conductivity at a temperature about 600°C and their stability in reducing atmosphere [4]. Barium cerates are known for their high protonic conductivity but are not chemically stable; they react with carbon dioxide to form carbonates. Barium zirconates are chemically and mechanically stable but their protonic conductivity is quite low [5–8]. An oxide with both cerium and zirconium could exhibit the two required properties for a PCFC electrolyte: a satisfying protonic conductivity and a sufficient stability [9, 10]. Thus, this study deals with $BaCe_{0.9-x}Zr_xY_{0.1}O_{3-\delta}$ powders ($x = 0.3$ (powder referred to BCZY63), $x = 0.7$ (BCZY27), and $x = 0.9$ (BCZY09)). The minimal value chosen for x was 0.3, because a compound with more than 60% of cerium atoms is not stable after a CO_2 treatment [10], and the lattice is orthorhombic. Kreuer [5] pointed out a decrease of the mobility of the protonic defects when the perovskite structures were deviating from cubic (orthorhombic). A trivalent dopant, yttrium, is used to create oxygen vacancies by charge compensation [2, 4, 11, 12]. These oxygen vacancies are necessary for the proton conduction, as explained afterwards.

Protons are incorporated in the material by the absorption of water molecules in the oxygen vacancies (reaction 1) [13–15].

Reaction 1

$$H_2O_{(g)} + V_O^{\bullet\bullet} + O_O^{x} \longleftrightarrow 2OH_O^{\bullet}. \quad (1)$$

Proton transfer occurs by the Grotthuss diffusion mechanism. This is a two-step mechanism which involves both a proton-transfer and a reorientation step [3, 15–18].

Cerates and Zirconates are pure proton conductors only at low temperature and under specific atmosphere. At high-oxygen partial pressure, p-type conduction is predominant (reaction 2).

Reaction 2

$$\frac{1}{2}O_{2(g)} + V_O^{\bullet\bullet} \longleftrightarrow 2h^{\bullet} + O_O^{x}. \quad (2)$$

Thus, the conductivity is given by (3) where σ_i is the ionic conductivity and $\sigma^{\circ}{}_p$ is the p-type conductivity at an oxygen partial pressure of 1 atm [4, 6, 19, 20] as follows:

$$\sigma_{\text{total}} = \sigma_i + \sigma^{\circ}{}_p \cdot P(O_2)^{1/4}. \quad (3)$$

2. EXPERIMENTAL

$BaCe_{0.9-x}Zr_xY_{0.1}O_{3-\delta}$ powders (x = 0.3, 0.7, and 0.9) were synthesized by a solid state reaction. $BaCO_3$ (Aldrich, 99+%), CeO_2 (Aldrich, 99.9%, <5 microns), Y_2O_3 (Sigma-Aldrich, 99.99%), and YSZ (Aldrich, submicron powder; 99.5%, 5.3 weight % of yttria) and were mixed in stoichiometric proportions for 20 hours in a ball mill. The resulting powders were calcined in air at 1400°C for 24 hours.

Crystallographic phases, lattice parameters, and theoretical density were determined with a standard X-ray diffractometer INEL CPS 120 using $Cu_{K\alpha 1}$ radiation.

Scanning Electron Microscope (SEM, Jeol JSM 6400F) experiments were achieved to assess the particles size and morphology.

2.1. Conventional sintering

A binder was added to the powders to facilitate the forming. Cylindrical pellets (10 and 20 mm diameter) were pressed using a hydraulic press (350 MPa) and sintered in air at 1700°C for 6 hours.

2.2. Spark plasma sintering

SPS was carried out in the equipment Sumitomo SPS 2080 supplied by (Plateforme Nationale de Frittage Flash (PNF2), Université Paul Sabatier, France). The precursors, without binding material, were set in graphite die with an inner diameter of 8 mm and sintered under vacuum (roughly 1 Pa). The experiments were done in the temperature range 1600–1700°C for 5 minutes. The pressure was monitored at 100 MPa during the process. The heating rate for all SPS experiments was maintained at around 150°C min^{-1}, and the natural cooling rate down to 800°C was 100°C min^{-1}. The temperature was controlled by an optical pyrometer focused on a small hole located at the surface of the die. Shrinkage was recorded from the dilatometer provided with the SPS machine.

The DC conductivity was measured in a 4-point probe arrangement. Pt paste was applied to each end of the bar and contacted with Pt leads. Two Pt potential probes at a fixed distance were set on one side of the bar, as shown in Figure 1. Different oxygen pressures were obtained by mixing O_2 and N_2 (oxidizing atmosphere), or H_2 and N_2 (reducing atmosphere). The gas mixture was moisturized by bubbling through water held at 13°C, giving a water-vapour partial pressure of ca. 0.015 atm. The isotope effect was measured by using D_2 and D_2O in place of H_2 and H_2O. The conductivity values were not corrected for the porosity of the samples.

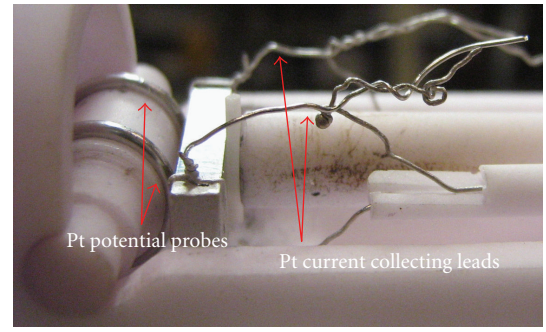

Figure 1: DC equipment.

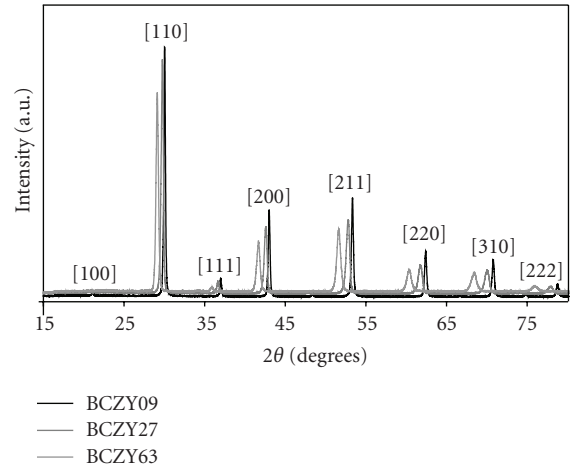

Figure 2: X-Ray patterns for BCZY09, BCZY27 and BCZY63 powders.

Table 1: BCZY powders lattice parameter and density.

Powder	Lattice parameter (Å)	Density (g·cm^{-3})
BCZY09	4.199	6.152
BCZY27	4.242	6.207
BCZY63	4.331	6.232

3. RESULTS AND DISCUSSION

3.1. Synthesized powders

The BCZY powders are single-phased and the structure is cubic (Figure 2). A 24-hour dwell is necessary to complete the reaction. Previous syntheses were achieved with a 12-hour dwell, and peaks of the precursors were present in the X-Ray patterns.

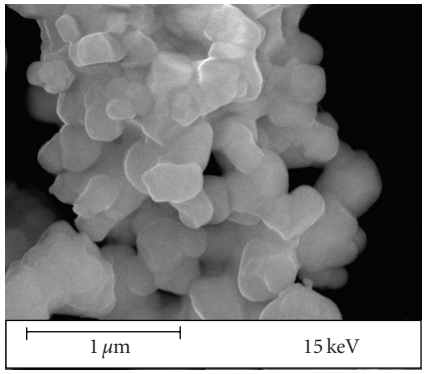

Figure 3: SEM picture of the BCZY27 powder.

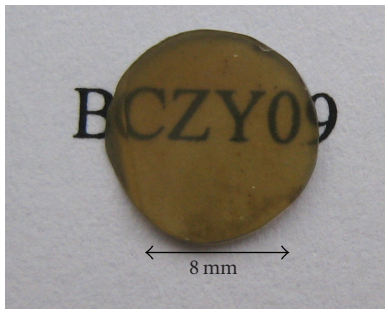

Figure 4: Picture of the BCZY09 SPS pellet, after polishing.

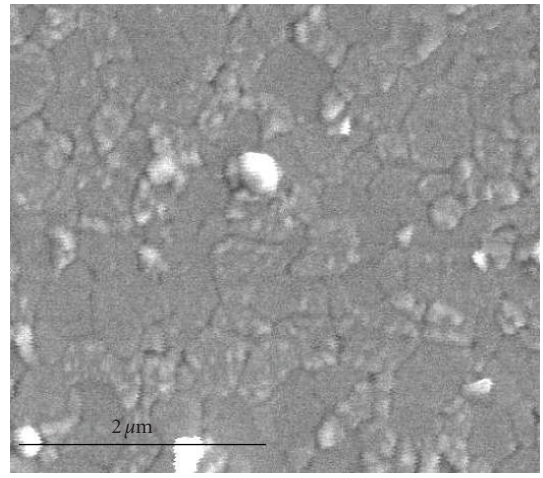

Figure 5: SEM picture of the BCZY09 SPS pellet, after a thermal etching.

Table 2: Fitted parameters $(\sigma i)_{H_2O}$, $(\sigma i)_{D_2O}$, and $\sigma^{\circ}{}_p$ for BCZY09 bars (SPS and CS) at 800°C.

Sample	$(\sigma i)_{H_2O}$ (mS/cm)	$(\sigma i)_{D_2O}$ (mS/cm)	$\sigma^{\circ}{}_p$ (mS/cm)
BCZY09 (SPS)	4.33	2.66	58.25
BCZY09 (CS)	1.85	1.21	25.3

The results of the lattice parameter (refined with Celref software) and density are summarized in Table 1. The grains are polygonal and nanoscale (about 300 nm for each cerium and zirconium content) (Figure 3).

3.2. Sintered pellets

Measurements of the sample geometry and Archimede's method were run to determine the density. For the SPS pellets, the two values are similar; the open porosity is negligible. A heat treatment at 800°C in air is required to remove graphite from the surface of the pellet, followed by polishing. The BCZY09 pellets are nearly fully transparent (Figure 4), with a density percentage of 99%. An SEM picture was obtained after a thermal etching at 1300°C (Figure 5). The impurities are due to the polishing and the gold coating. The grain size is about 500 nm, and no crack is present on the pellet. The BCZY27 and BCZY63 samples disintegrated totally after a few days, revealing a difference of colors between the bulk and the superficial layers. XRD patterns were recorded on these broken pellets, after grinding: only the BCZY perovskite phase is present in the diffractogram. One hypothesis is the partial reduction of cerium ions because of the highly reductive atmosphere in the graphite die at high temperature. Ce^{3+} ions are larger than Ce^{4+} ions and mechanical stresses would be generated during the reduction.

The pellets made by conventional sintering at 1700°C present a high-open porosity (Figure 6). Indeed, the density percentage obtained by geometric measurements is about 80%, whereas the one obtained with Archimede's method is about 90%. Cracks and defects exist at the surface of the samples; the pressure is not homogeneously distributed during uniaxial pressing. An SEM picture is shown in Figure 7: the grains are irregular and bigger than the ones in the SPS pellet, between 500 nm and 1.5 μm. Furthermore, a change of the superficial color is obvious, due to an oxygen nonstoichiometry. Polishing is necessary to remove it. The X-ray patterns show the expected perovskite phase.

Conventional sintering in different atmosphere (synthetic air or argon) was tried to avoid this superficial coloration, but with no positive result.

DC experiments were tried at 600°C, but the really high density of the SPS sample required a very long equilibrium time (more than one day for each gas composition). So the DC curves were obtained at 800°C and are presented in Figure 8.

Equation (3) was adjusted to the conductivity data in both gas atmospheres and the parameters $(\sigma i)_{H_2O}$, $(\sigma i)_{D_2O}$, and $\sigma^{\circ}{}_p$ were determined [19, 20]. The results are summarized in Table 2. The difference between conductivity of D_2O and H_2O exchanged states shows the protonic component of the conductivity.

One can note a higher ionic contribution of the conductivity for the SPS sample, which can be partly related to the higher density. Grain boundaries in the SPS samples do not diffuse the light (transparent sample). These grain boundaries should present different properties than those of the pellet obtained by conventional sintering. Grain

Figure 6: Picture of the BCZY09 CS pellet, after polishing.

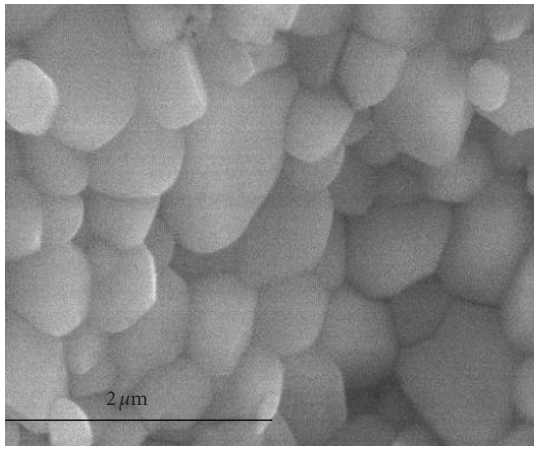

Figure 7: SEM picture of the BCZY09 CS pellet.

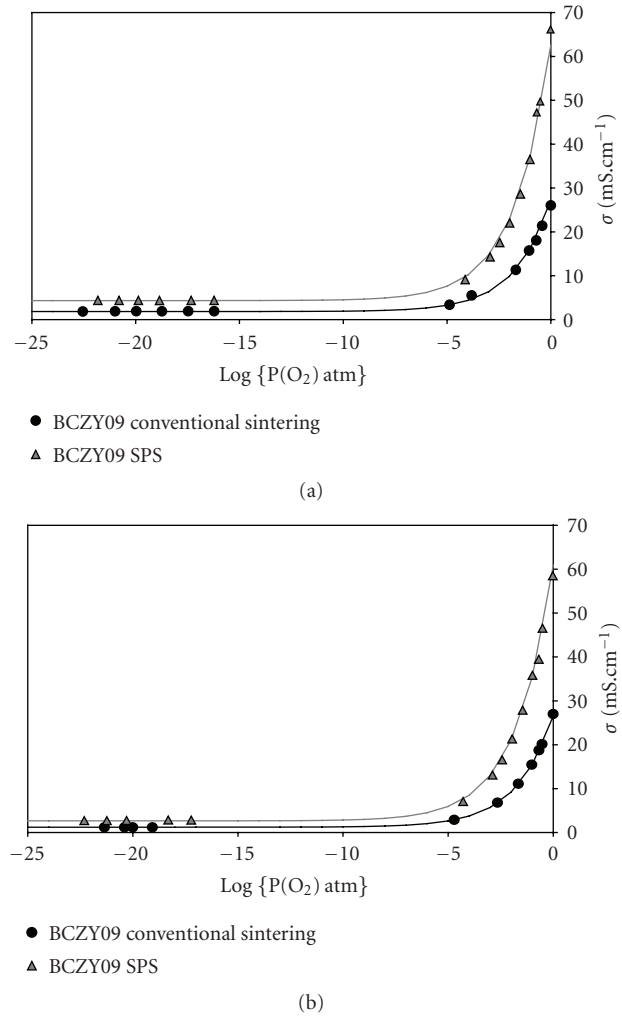

Figure 8: DC curves at 800°C for H_2O exchanged state (a) and D_2O exchange state (b).

boundaries contribute to the total conductivity of the sample. So, this could also explain the difference of ionic conductivity of the two samples.

The p-type conductivity is also higher for the SPS sample. The highly reductive atmosphere at 1700°C creates holes. The fast cooling does not let enough time for the reoxidation step. Holes are trapped in the material, generating higher p-type conductivity.

4. FUTURE WORK

Three different sets of experiment will be run to complete this study. First, different temperature dwells, and cooling rates will be tested to investigate the influence on the mechanical stress releases. Then, different atmospheres can be used during the SPS sintering. This will modify the reductive property in the graphite die at high temperature. Finally, the influence of the grain boundaries on the total conductivity will be determined by impedance spectra at low temperature with silver electrodes.

5. CONCLUSIONS

BCZY compounds can be synthesized by a solid-state reaction, with a 24-hour dwell at 1400°C. The XRD analyses reveal a cubic perovskite structure. The sintering can be achieved by a conventional way, with a 6-hour dwell at 1700°C, followed by a fast surface polishing. To reduce the superficial defects, isostatic pressing should be achieved.

To increase the density percentage, SPS experiments can be run. When cerium is present in the sample, the pellet disintegrates. Other SPS procedures (different temperature dwells, cooling rates, and atmospheres) are now studied to obtain stable BCZY27 and BCZY63 pellets. The SPS method is very promising because of the high-densified crackless samples obtained.

Conductivity measurements were run on BCZY09 bars. The higher ionic component of the conductivity for the SPS sample is beneficial to use the material as electrolyte for PCFC. The p-type conductivity is also higher for the SPS bar. This can be changed with a slower cooling rate allowing a reoxidation of the sample.

REFERENCES

[1] D. W. Lee, J. H. Won, and K. B. Shim, "Low temperature synthesis of $BaCeO_3$ nano powders by the citrate process," *Materials Letters*, vol. 57, no. 22-23, pp. 3346–3351, 2003.

[2] K. Künstler, H.-J. Lang, A. Maiwald, and G. Tomandl, "Synthesis, structure and electrochemical properties of In-doped $BaCeO_3$," *Solid State Ionics*, vol. 107, no. 3-4, pp. 221–229, 1998.

[3] W. Münch, K.-D. Kreuer, G. Seifert, and J. Maier, "Proton diffusion in perovskites: comparison between $BaCeO_3$, $BaZrO_3$, $SrTiO_3$, and $CaTiO_3$ using quantum molecular dynamics," *Solid State Ionics*, vol. 136-137, pp. 183–189, 2000.

[4] N. Bonanos, "Oxide-based protonic conductors: point defects and transport properties," *Solid State Ionics*, vol. 145, no. 1–4, pp. 265–274, 2001.

[5] K. D. Kreuer, "Aspects of the formation and mobility of protonic charge carriers and the stability of perovskite-type oxides," *Solid State Ionics*, vol. 125, no. 1–4, pp. 285–302, 1999.

[6] N. Bonanos, K. S. Knight, and B. Ellis, "Perovskite solid electrolytes: structure, transport properties and fuel cell applications," *Solid State Ionics*, vol. 79, pp. 161–170, 1995.

[7] M. J. Scholten, J. Schoonman, J. C. van Miltenburg, and E. H. P. Cordfunke, "The thermodynamic properties of $BaCeO_3$ at temperatures from 5 to 940 K," *Thermochimica Acta*, vol. 268, pp. 161–168, 1995.

[8] T. Shimada, C. Wen, N. Taniguchi, J. Otomo, and H. Takahashi, "The high temperature proton conductor $BaZr_{0.4}Ce_{0.4}In_{0.2}O_{3-\alpha}$," *Journal of Power Sources*, vol. 131, no. 1-2, pp. 289–292, 2004.

[9] K. H. Ryu and S. M. Haile, "Chemical stability and proton conductivity of doped $BaCeO_3$-$BaZrO_3$ solid solutions," *Solid State Ionics*, vol. 125, no. 1–4, pp. 355–367, 1999.

[10] K. Katahira, Y. Kohchi, T. Shimura, and H. Iwahara, "Protonic conduction in Zr-substituted $BaCeO_3$," *Solid State Ionics*, vol. 138, no. 1-2, pp. 91–98, 2000.

[11] T. Schober, F. Krug, and W. Schilling, "Criteria for the application of high temperature proton conductors in SOFCs," *Solid State Ionics*, vol. 97, no. 1–4, pp. 369–373, 1997.

[12] I. Kosacki and H. L. Tuller, "Mixed conductivity in $SrCe_{0.95}Yb_{0.05}O_3$ protonic conductors," *Solid State Ionics*, vol. 80, no. 3-4, pp. 223–229, 1995.

[13] H. Iwahara, "Proton conducting ceramics and their applications," *Solid State Ionics*, vol. 86–88, part 1, pp. 9–15, 1996.

[14] Ph. Colomban, "Latest developments in proton conductors," *Annales de Chimie Science des Matériaux*, vol. 24, no. 1, pp. 1–18, 1999.

[15] A. S. Nowick and Y. Du, "High-temperature protonic conductors with perovskite-related structures," *Solid State Ionics*, vol. 77, pp. 137–146, 1995.

[16] T. Norby, "Solid-state protonic conductors: principles, properties, progress and prospects," *Solid State Ionics*, vol. 125, no. 1–4, pp. 1–11, 1999.

[17] R. Hempelmann, "Hydrogen diffusion mechanism in proton conducting oxides," *Physica B*, vol. 226, no. 1–3, pp. 72–77, 1996.

[18] N. Agmon, "The Grotthuss mechanism," *Chemical Physics Letters*, vol. 224, no. 5-6, pp. 456–462, 1995.

[19] Y. Larring and T. Norby, "Protons in $LaErO_3$," *Solid State Ionics*, vol. 70-71, part 1, pp. 305–310, 1994.

[20] D. Lybye and N. Bonanos, "Proton and oxide ion conductivity of doped $LaScO_3$," *Solid State Ionics*, vol. 125, no. 1–4, pp. 339–344, 1999.